

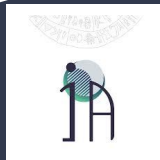
The first unbiased survey of star-forming galaxies with eROSITA:

Scaling relations and a population of X-ray luminous starbursts

Elias Kyritsis
University of Crete
Institute of Astrophysics- FORTH



Andreas Zezas, Frank Haberl, Joern Wilms, Philipp Weber, Steven Hämmerich,
Manami Sasaki, Ann Hornschemeier, Antara Basu-Zych, Roman Laktionov,
Neven Vulic, Andy Ptak, Andrea Merloni
& the eROSITA Normal Galaxies WG



"First Results from the SRG/eROSITA All-Sky Survey: From Stars to Cosmology"
September 20th 2024, Garching, Germany



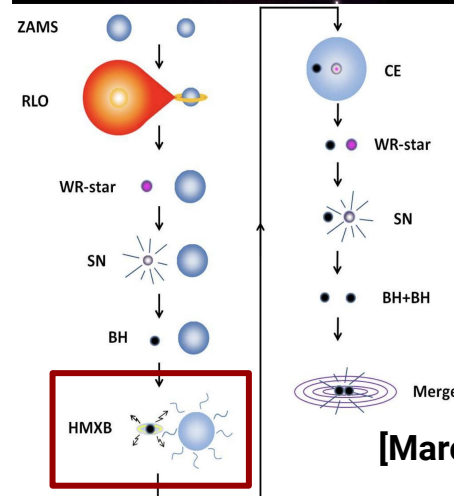
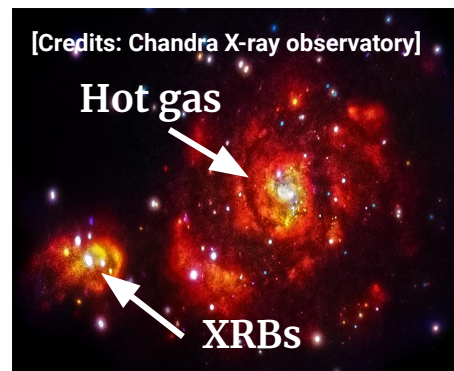
Studying the X-ray output of Normal Galaxies in the local Universe

X-ray emission of normal galaxies is produced by:

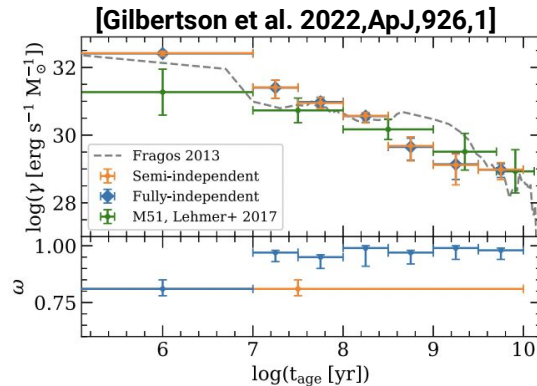
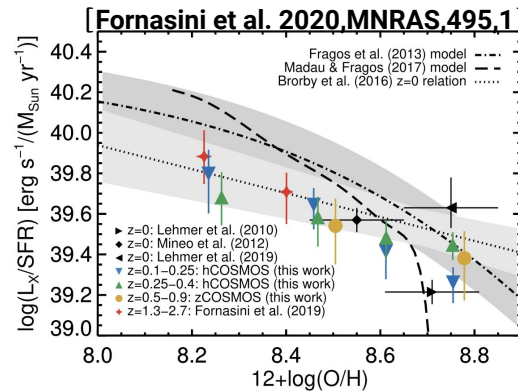
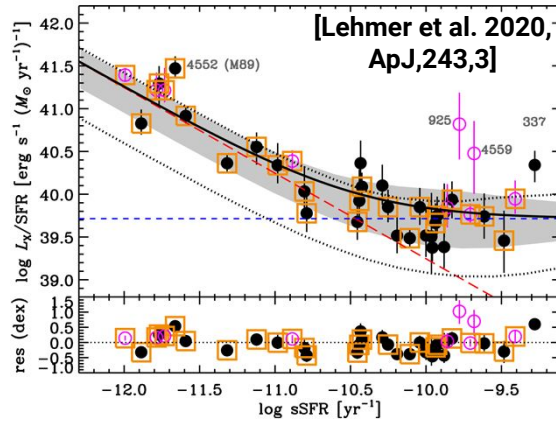
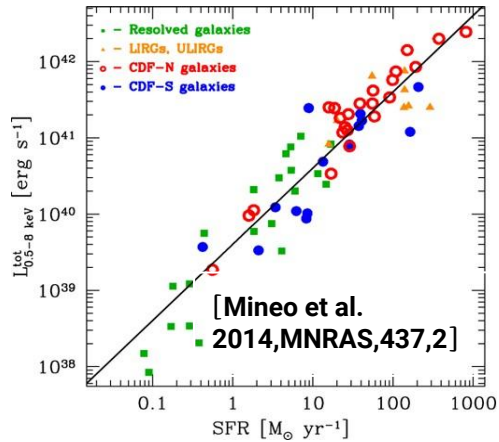
X-ray Binaries (XRBs) & hot gas.

- ❖ **Constrain the evolutionary parameters** of XRBs by testing **different evolution scenaria** through population synthesis.
 - Orbital parameters, mass ratios
 - Stellar winds, SN kicks, CE ejection
- ❖ **Predict the formation rate** of GWs and/or sGRBs.
- ❖ **Study the effect of XRBs** on their **host galaxy** & the surrounding **IGM**.
- ❖ Study the **cosmological evolution of galaxies**.
 - First XRBs may affect the formation of the first galaxies in the Universe

L_x - SFR - M_{\star} - Metallicity scaling relations



Current state of the art & limitations



Current observational constraints

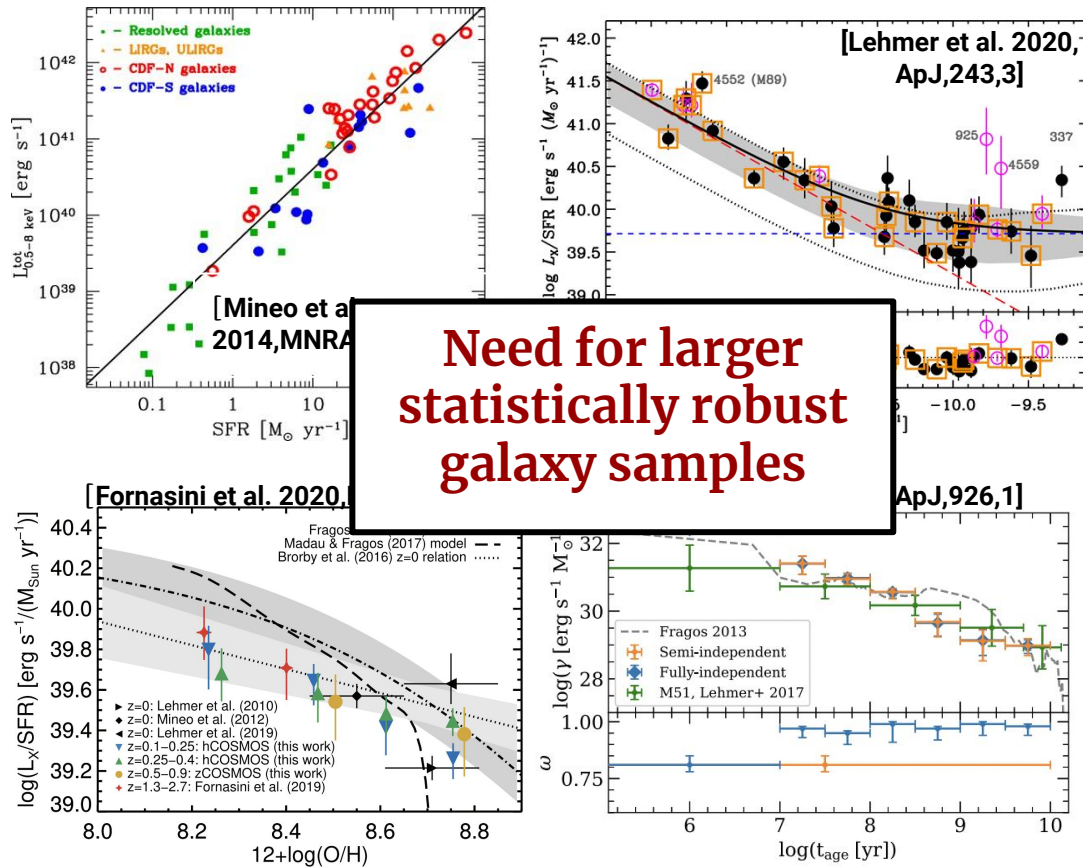
- ❖ X-ray output as a function of: **SFR**, M_{\star} , **Metallicity**
- ❖ Increased L_x correlates with:
 - Metallicity
 - Age of the stellar populations

However...

Based on limited, non-representative samples.

Small coverage of the **SFR**- M_{\star} -**Metallicity** parameter space from specially selected galaxy samples.

Current state of the art & limitations



Need for larger statistically robust galaxy samples

Current observational constraints

- ❖ X-ray output as a function of: **SFR**, M_{\star} , **Metallicity**
- ❖ Increased L_x correlates with:
 - Metallicity
 - Age of the stellar populations

However...

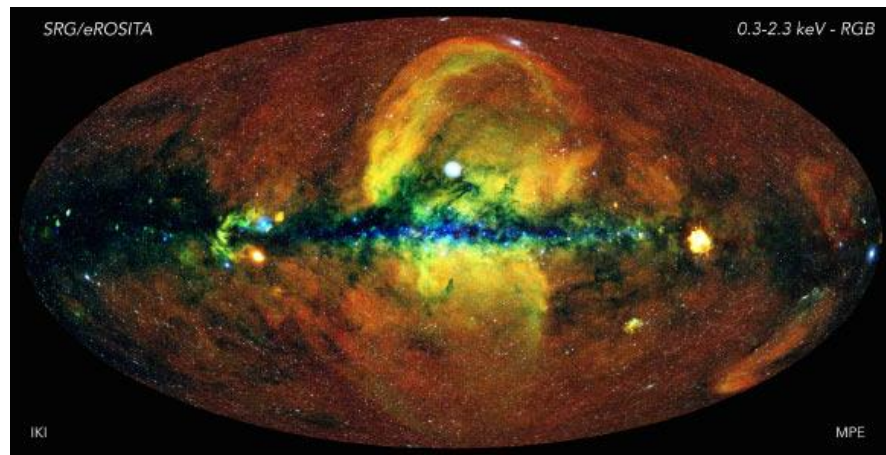
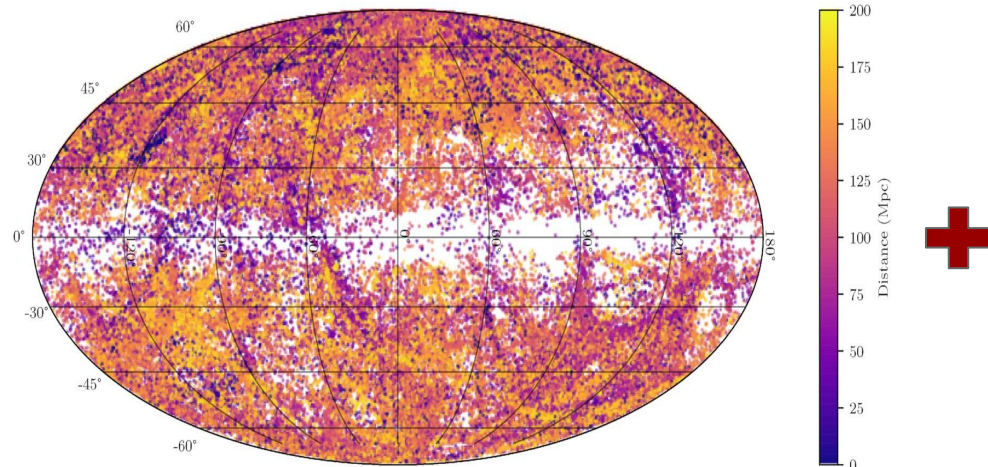
Based on limited, non-representative samples.

Small coverage of the **SFR**- M_{\star} -**Metallicity** parameter space from specially selected galaxy samples.

HECATEv2 + eRASS1: X-ray all sky survey

[Kovlakas et al. 2021, MNRAS, 506, 2; Kyritsis et al. in prep.]

[Predehl et al. 2021, A&A 647, A1; Merloni et al. 2024, A&A, 687, A34]



204733 galaxies at distance up to 200 Mpc ($z \sim 0.048$)

- ✓ **Basic properties:** position, Distance, Size
- ✓ **Multi-wavelength data:** IR to Optical photometry & SDSS spectroscopic information
- ✓ **Stellar population parameters:** SFR, M_{\star} , Metallicity
- ✓ **Activity classification:** Star-Forming, AGN, Composite, LINER, Passive

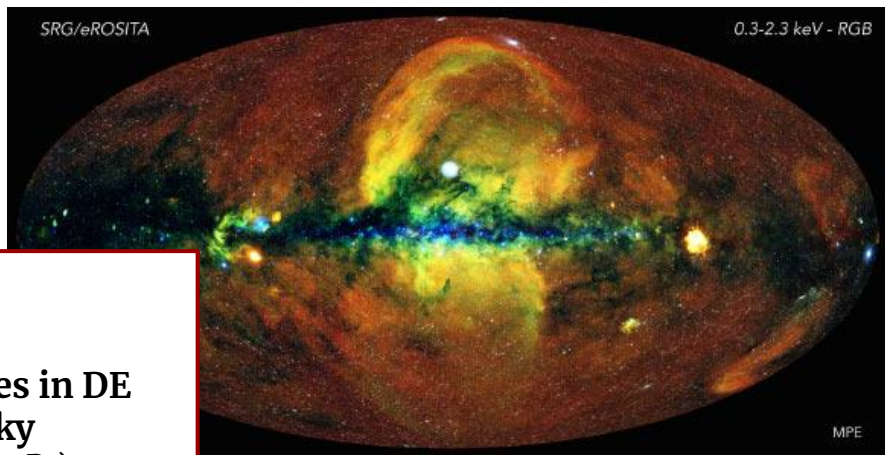
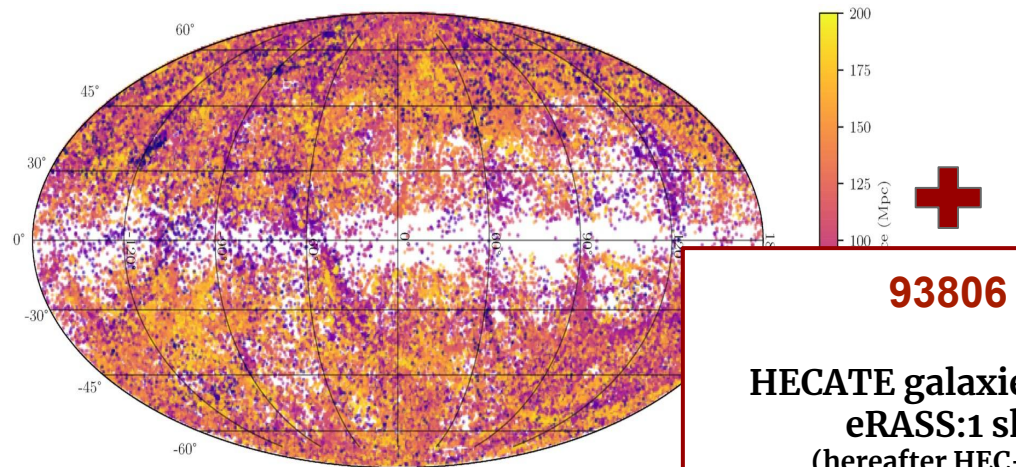
Table 6. Summary of performance characteristics of the eROSITA telescope and its survey sensitivity.

		Energy range	
		Soft band	Hard band
		0.2–2.3 keV	2.3–8 keV
FoV averaged effective area [cm^2]		1237 at 1 keV	139 at 5 keV
Total background [$10^{-3} \text{ cts s}^{-1} \text{ arcmin}^{-2}$]		≈ 3.7	≈ 2.1
<i>Point source sensitivity eRASS:1</i>			
Ecliptic Equatorial region	Total exposure = 200 s	$5 \times 10^{-14} \text{ erg s}^{-1} \text{ cm}^{-2}$	$7 \times 10^{-13} \text{ erg s}^{-1} \text{ cm}^{-2}$
Ecliptic Polar region	Total exposure = 4000 s	$7 \times 10^{-15} \text{ erg s}^{-1} \text{ cm}^{-2}$	$9 \times 10^{-14} \text{ erg s}^{-1} \text{ cm}^{-2}$
<i>Point source sensitivity eRASS:1-8 (predicted)</i>			
Ecliptic Equatorial region	Total exposure = 1600 s	$1.1 \times 10^{-14} \text{ erg s}^{-1} \text{ cm}^{-2}$	$2.5 \times 10^{-13} \text{ erg s}^{-1} \text{ cm}^{-2}$
Ecliptic Polar region	Total exposure = 30000 s	$2.5 \times 10^{-15} \text{ erg s}^{-1} \text{ cm}^{-2}$	$4 \times 10^{-14} \text{ erg s}^{-1} \text{ cm}^{-2}$

HECATE + eRASS1: X-ray all sky survey

[Kovlakas et al. 2021, MNRAS, 506, 2; Kyritsis et al. in prep.]

[Predehl et al. 2021, A&A 647, A1; Merloni et al. 2024, A&A, 687, A34]



93806
HECATE galaxies in DE
eRASS:1 sky
(hereafter HEC-eR1)

Performance characteristics of the eROSITA telescope and its survey sensitivity.

204733 galaxies at distance up to 200 Mpc ($z \sim 0.048$)

- ✓ **Basic properties:** position, Distance, Size
- ✓ **Multi-wavelength data:** IR to Optical photometry & SDSS spectroscopic information
- ✓ **Stellar population parameters:** SFR, M_{\star} , Metallicity
- ✓ **Activity classification:** Star-Forming, AGN, Composite, LINER, Passive

		Energy range	
		Soft band	Hard band
		0.2–2.3 keV	2.3–8 keV
FoV averaged effective area [cm ²]		1237 at 1keV	139 at 5 keV
Total background [10 ⁻³ cts s ⁻¹ arcmin ⁻²]		≈3.7	≈2.1
<i>Point source sensitivity eRASS:1</i>			
Ecliptic Equatorial region	Total exposure = 200 s	5×10^{-14} erg s ⁻¹ cm ⁻²	7×10^{-13} erg s ⁻¹ cm ⁻²
Ecliptic Polar region	Total exposure = 4000 s	7×10^{-15} erg s ⁻¹ cm ⁻²	9×10^{-14} erg s ⁻¹ cm ⁻²
<i>Point source sensitivity eRASS:1-8 (predicted)</i>			
Ecliptic Equatorial region	Total exposure = 1600 s	1.1×10^{-14} erg s ⁻¹ cm ⁻²	2.5×10^{-13} erg s ⁻¹ cm ⁻²
Ecliptic Polar region	Total exposure = 30000 s	2.5×10^{-15} erg s ⁻¹ cm ⁻²	4×10^{-14} erg s ⁻¹ cm ⁻²

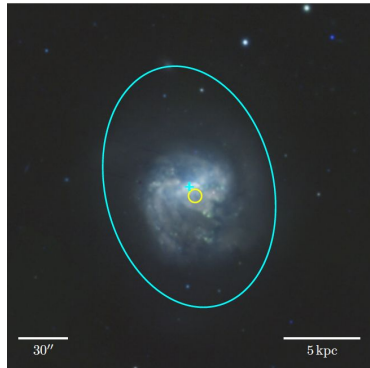
HEC -eR1: Normal Galaxy study

Methodology - X-ray photometry

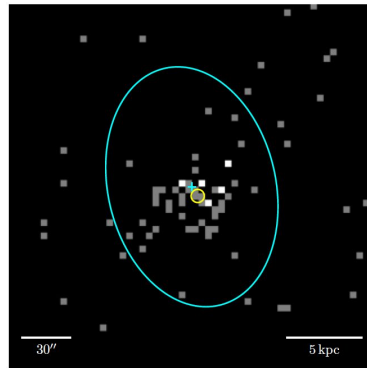
93806 HEC-eR1 galaxies

1. Extracted X-ray spectra

- Accounting for extended emission;
P. Weber, S. Hämmerich



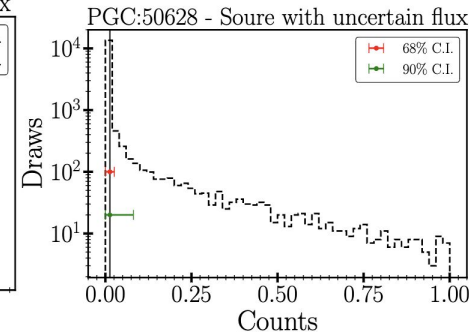
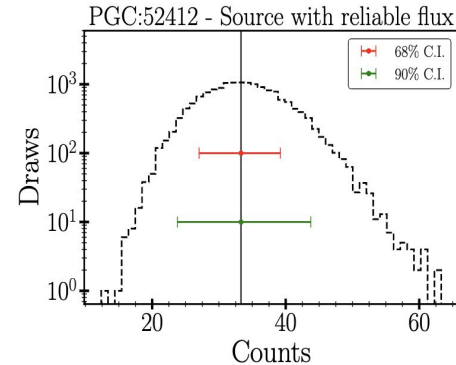
PanSTARRS



eRASS1 0.2-5 keV

2. Measurement of source intensity

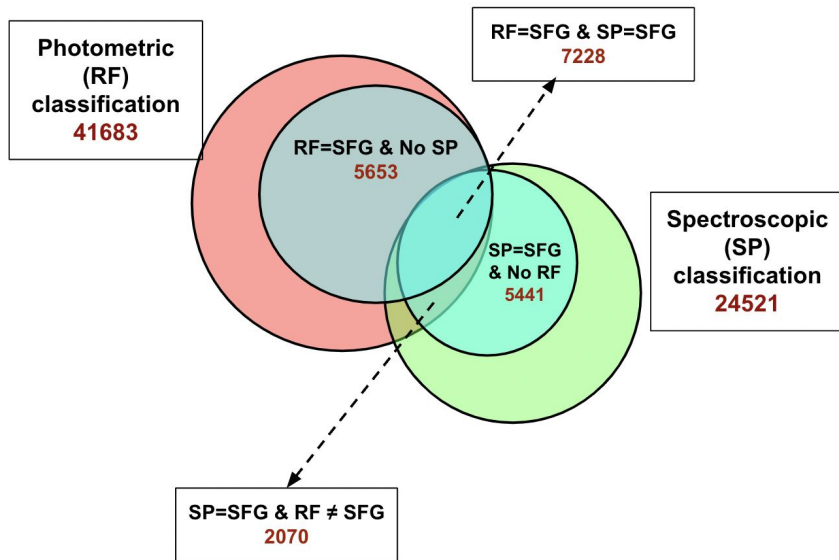
- Posterior probability of the source's intensity
- BEHR (Bayesian approach)



- ### 3. Calculate **Flux & Luminosity** based on the Posterior of the source's intensity and the distance of each galaxy.

HEC-eR1 sample construction

Selection of star-forming galaxies



Final Sample after screening

Reliable fluxes : **78**

Unreliable fluxes (Upper Limits): **18792**

Total: 18870 star-forming galaxies

Activity classification methods

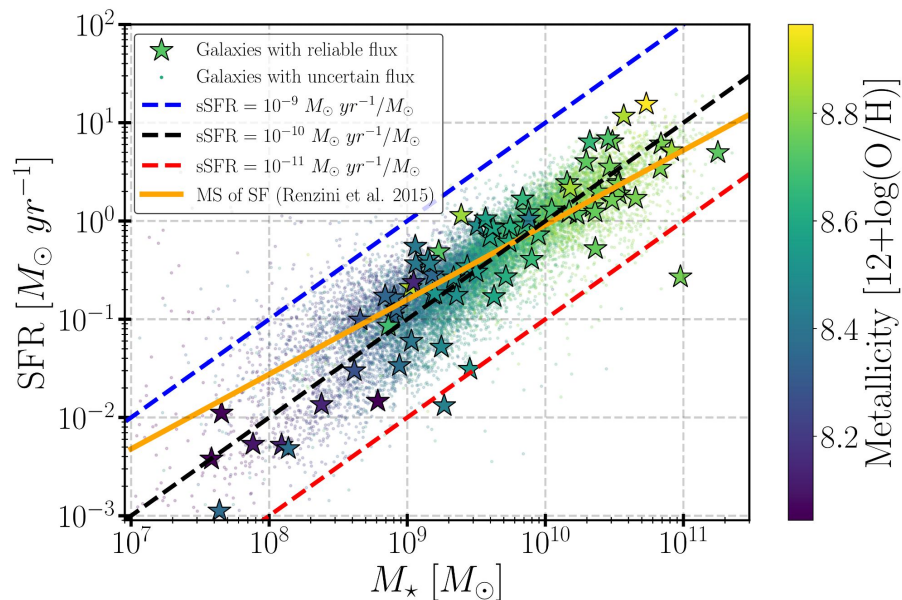
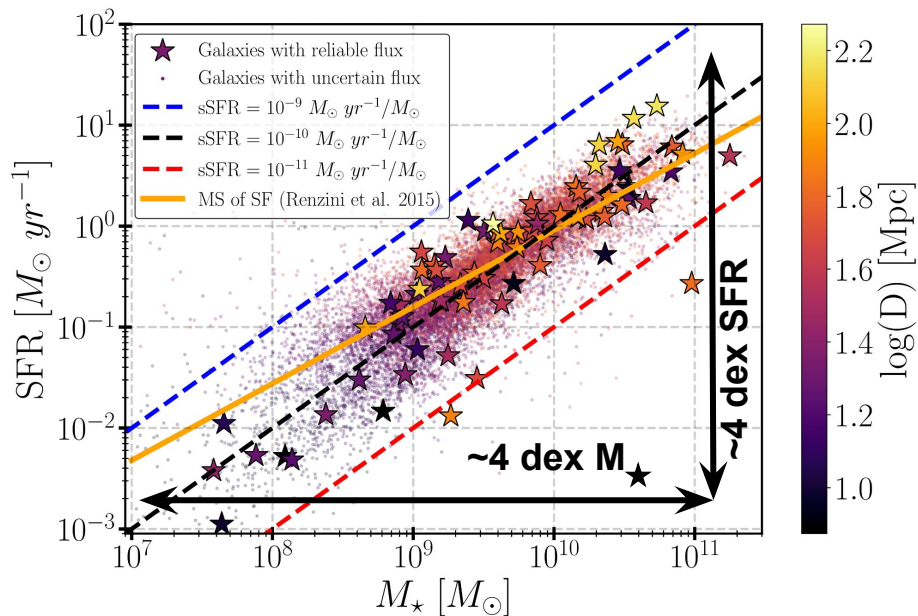
- ❖ Spectroscopic (SP) data (SDSS+Skinakas/TNG). [Stampoulis et al., A&A, 2019,486]
- ❖ Photometric mid-IR/optical data (RF).
 - **5-class activity classifier based on Random Forest machine learning algorithm** [C.Daoutis, E. Kyritsis et al., A&A,2023,679:A76]

AGN & Galaxy Cluster screening

- AGN contamination (visual inspection; literature search)
- Hot-gas contamination from Galaxy Clusters
 - eROSITA Galaxy Cluster catalog (F.Harbel, E.Bulbul)
 - Abell Cluster catalog
 - Hickson Compact Group Galaxy
- UVOIR variability:
 - Cross-match with a sample of AGN identified by their UVOIR variability observed with eROSITA (Arcodia et al.2024, A&A, 681, A97)
- Hard X-ray colors

HEC-eR1 final sample of star-forming galaxies

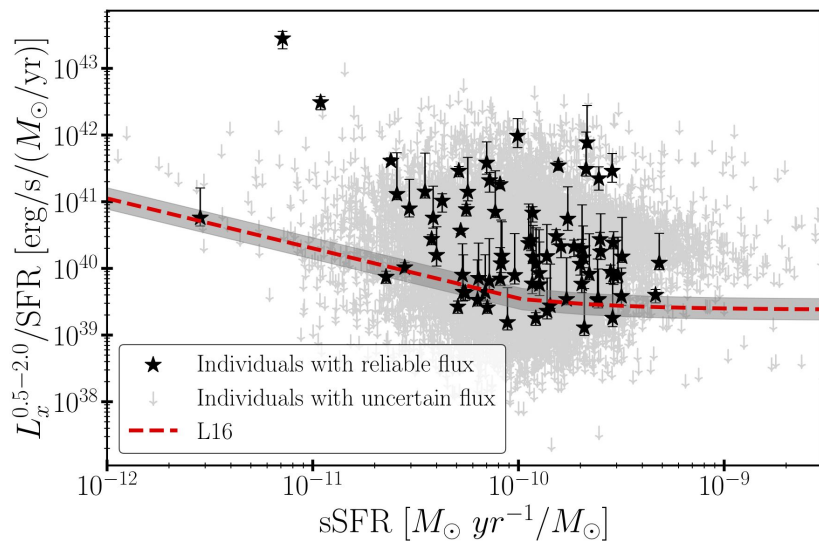
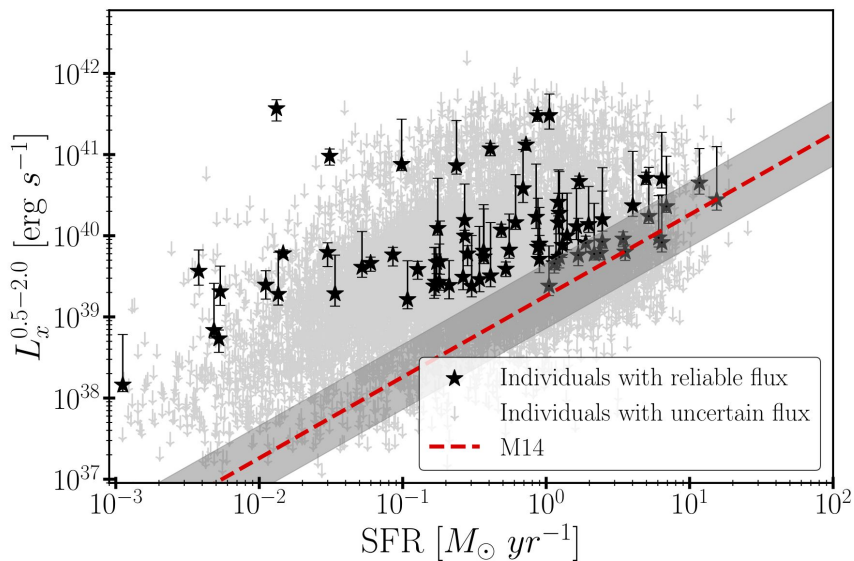
SFR- M_{\star} -D-Metallicity parameter space



Our sample is **well distributed in the galaxy Main Sequence plane** and it covers a wide range of **sub-solar to super-solar metallicities**.

HEC-eR1 Normal Galaxy study

Scaling relations of individual galaxies



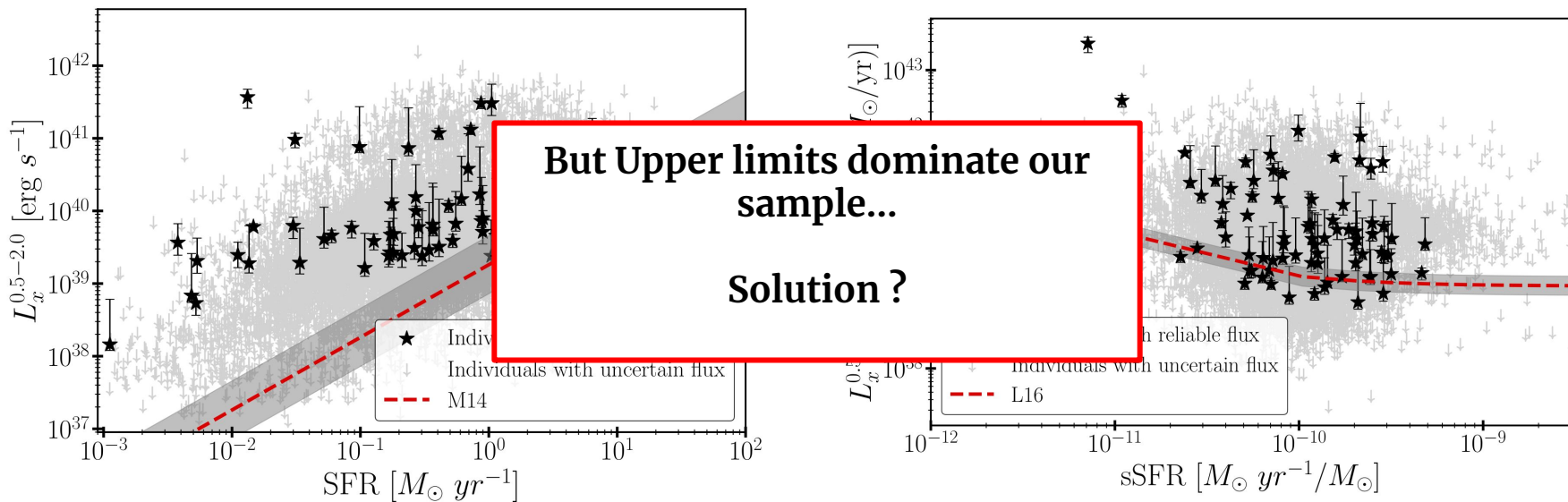
➤ A population of extremely X-ray luminous galaxies is systematically above the L_x -SFR (M14) & L_x -SFR- M_\star (L16) scaling relations !

➤ Increased scatter !

➤ Increased deviations for low SFRs !

HEC-eR1 Normal Galaxy study

Scaling relations of individual galaxies



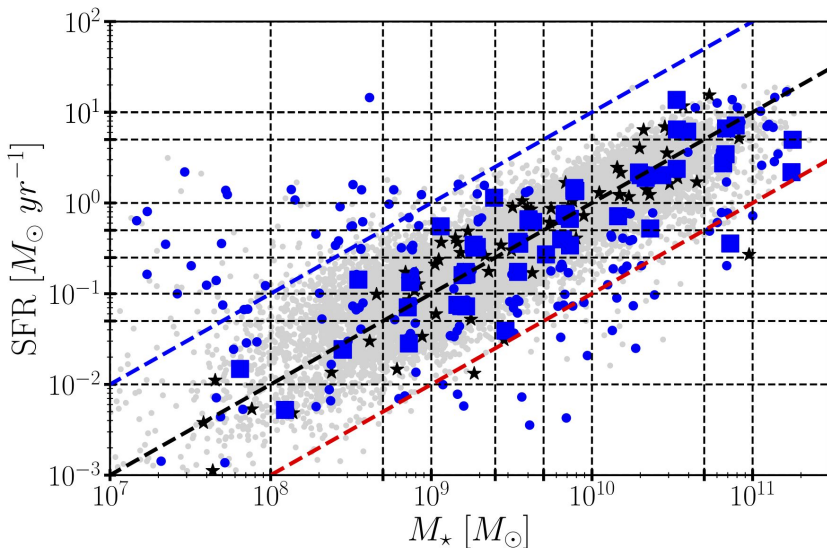
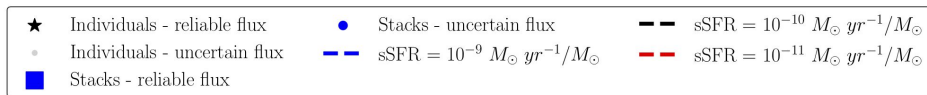
➤ A population of extremely X-ray luminous galaxies is systematically above the L_x-SFR (M14) & L_x-SFR- M_\star (L16) scaling relations !

➤ Increased scatter !

➤ Increased deviations for low SFRs !

HEC-eR1 Normal Galaxy study

Stacking the galaxies per SFR - M_{\star} - D bin

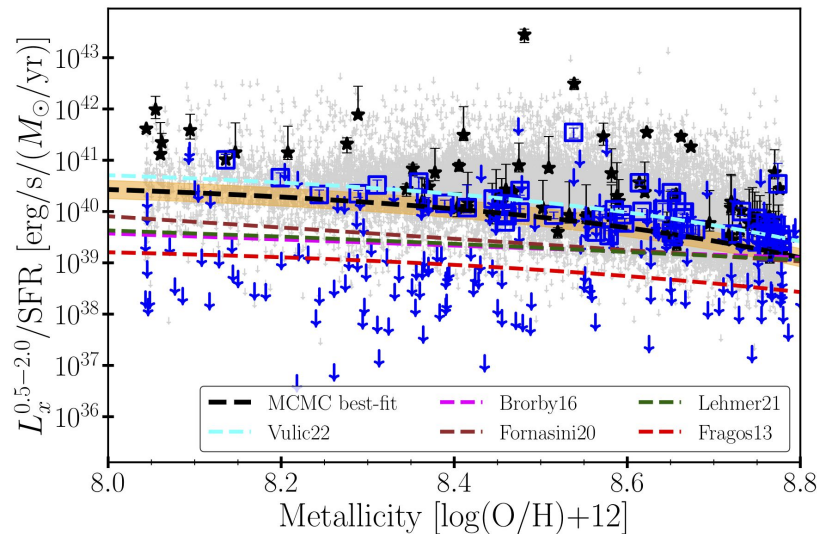
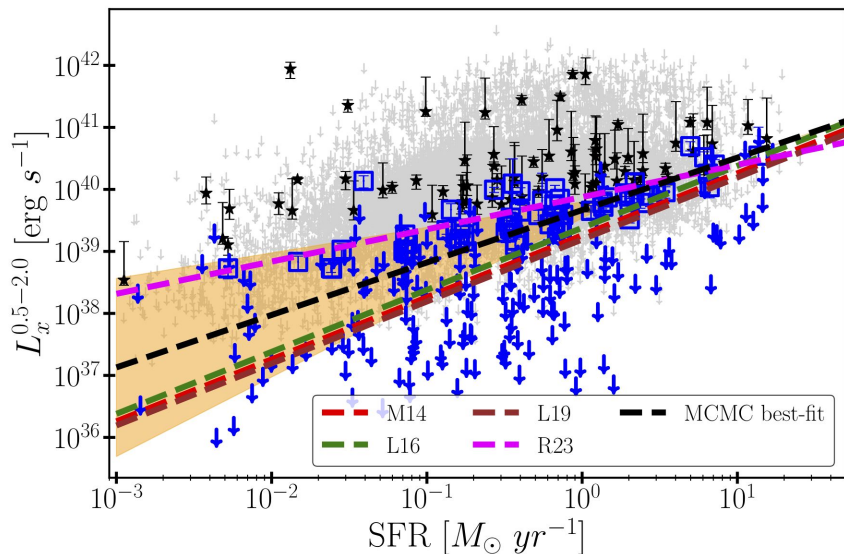


SFR- M_{\star} - D grid : **10x11x9**

- Select all the galaxies per bin following an adaptive binning: **239** bins
- **Reliable: 58** bins & **Upper limits: 181** bins
- Calculation of the $\langle Lx \rangle$ of the galaxy population per SFR- M_{\star} -D bin

HEC-eR1 Normal Galaxy study

Updated L_X -SFR & L_X -SFR-Metallicity scaling relations



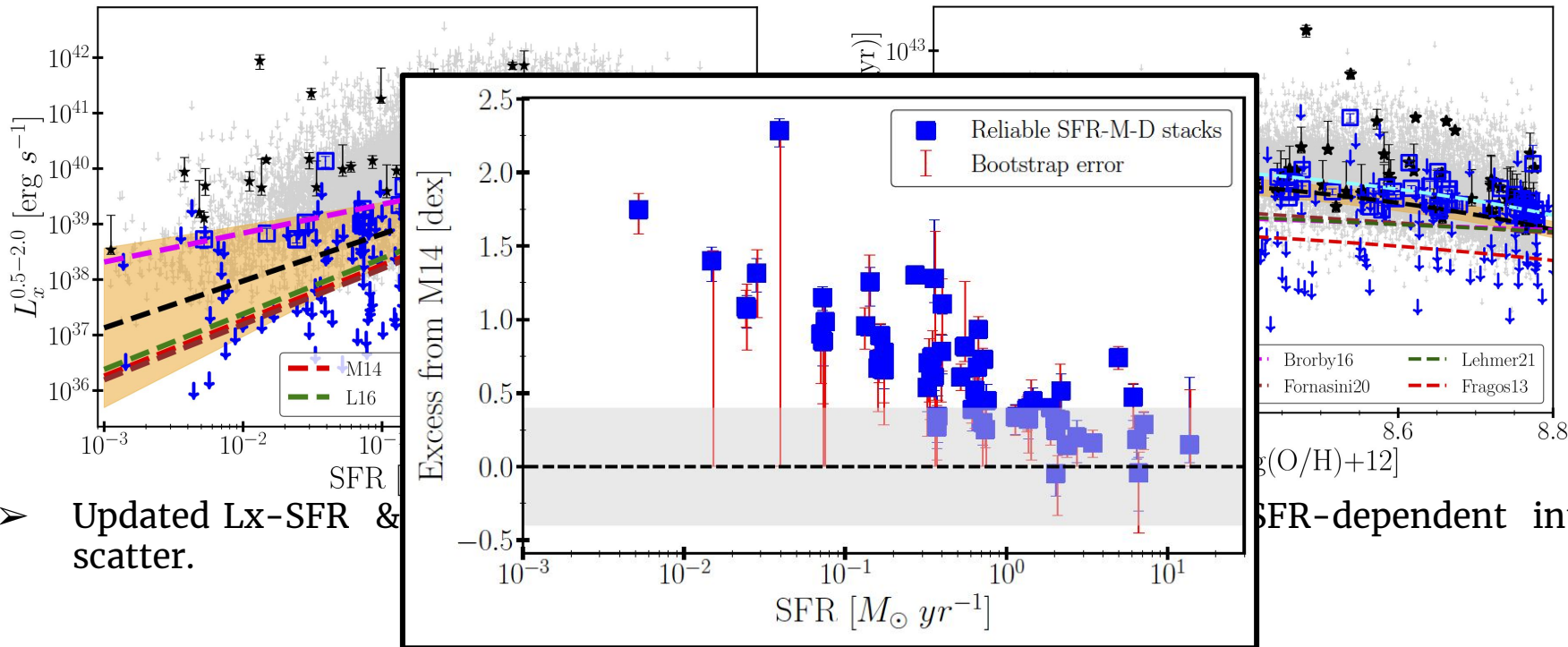
- Updated L_X -SFR & L_X -SFR-Z accounting for the Upper limits & the SFR-dependent intrinsic scatter.

$$\log(L_X/\text{erg s}^{-1}) = A \cdot \log(\text{SFR}/M_\odot \text{ yr}^{-1}) + B + \epsilon(\log(\text{SFR}))$$

$$\log(L_X/\text{erg s}^{-1}) = \log(\text{SFR}/M_\odot \text{ yr}^{-1}) + A \cdot (Z/Z_\odot) + B + \sigma$$

HEC-eR1 Normal Galaxy study

Updated L_x -SFR & L_x -SFR-Metallicity scaling relations



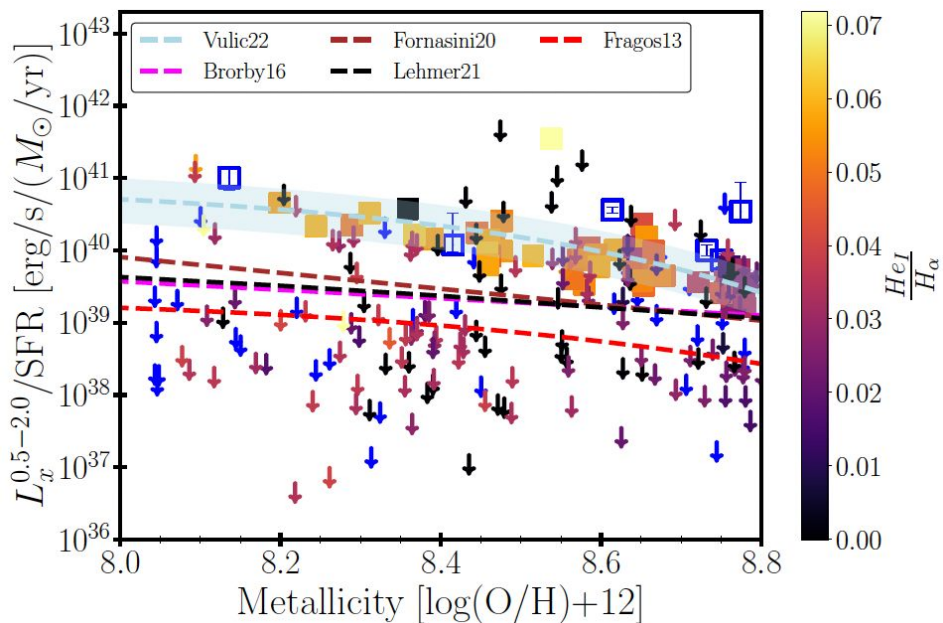
➤ Updated L_x -SFR & scatter.

➤ The excess persists ! Stronger towards lower SFRs & higher sSFRs.

- Up to **~ 2 dex** for **$\text{SFR} < 0.01 M_\odot/\text{yr}$** .
- Scatter **correlates** with SFR

HEC-eR1 Normal Galaxy study

Lx excess: Stellar population age or Metallicity?



Partial correlation test accounting for the upper limit stacks .

- **Lx/SFR excess - Metallicity** → control for **HeI/H α**
 - Low variance
- **Lx/SFR excess - HeI/H α** → control for **Metallicity**
 - High variance

Stellar age is more strongly correlated with the Lx excess for stellar populations of age up to ~30 Myrs !

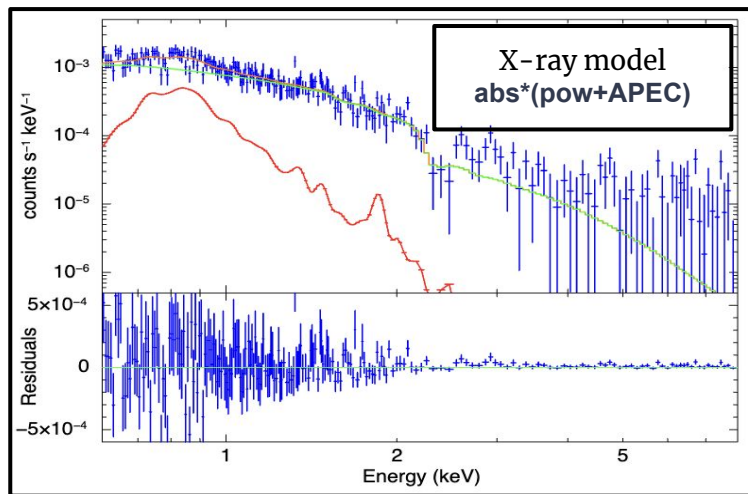
- ❖ HeI/5876 traces stellar populations of <8 Myrs
- ❖ H α /6563 traces stellar populations of <30 Myrs

HEC-eR1 Normal Galaxy study

Lx excess: Hot-gas contribution or LMXBs ?

Is the excess due to hot-gas contribution ?

$$\text{Hot-gas contribution} = \frac{F_{0.5-2}^{\text{APEC}}}{F_{0.5-2}^{\text{total}}} \times 100 \% = \sim 13 \%$$

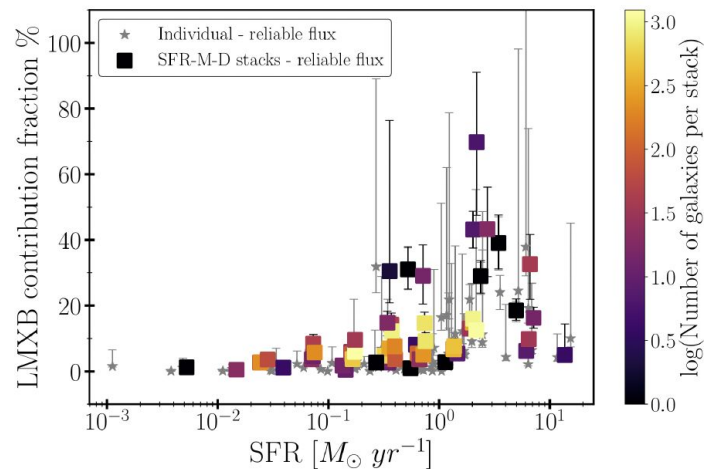


➤ Consistent with other works using eRASS4 data [Laktionov et al. 2024 in prep., See poster]

★ Cannot explain the excess we measure.

Is the excess at lower SFRs due to the contribution of the LMXBs in the integrated Lx ?

➤ Calculate the expected Lx based on LMXBs XLF from Lehmer+19

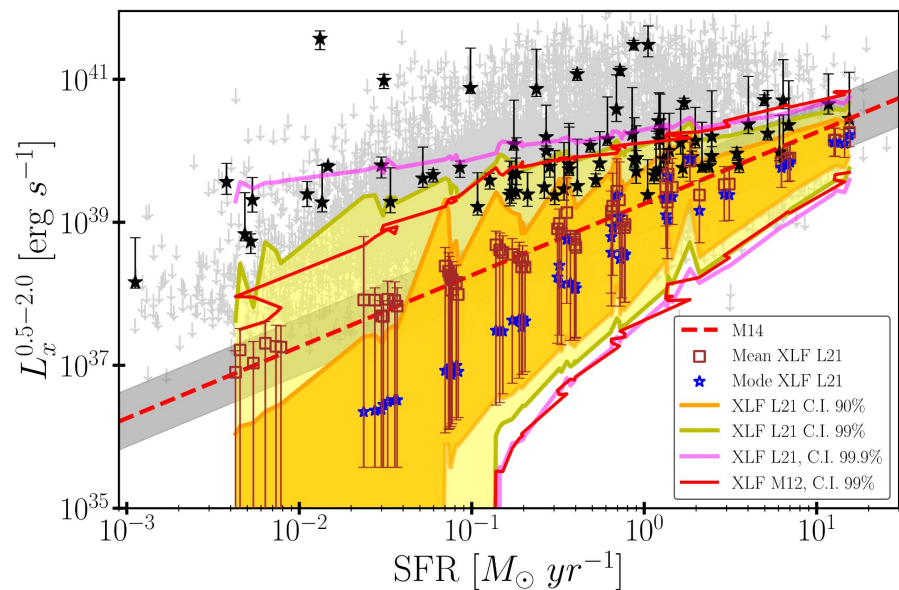


★ LMXBs cannot explain the excess in lower SFRs.

HEC-eR1 Normal Galaxy study

Lx excess: Stochasticity effect ?

Has the $\langle L_x \rangle$ excess a physical origin or it is the result of the stochastic sampling of the HMXBs XLF ?



➤ Simulation of the expected L_x distribution due to stochastic sampling of HMXBs XLFs.

- Solar-metallicity Mineo+12 (M12)
- Metallicity-dependent Lehmer+21 (L21)

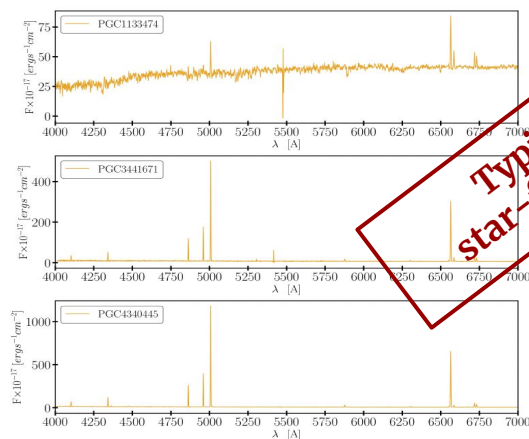
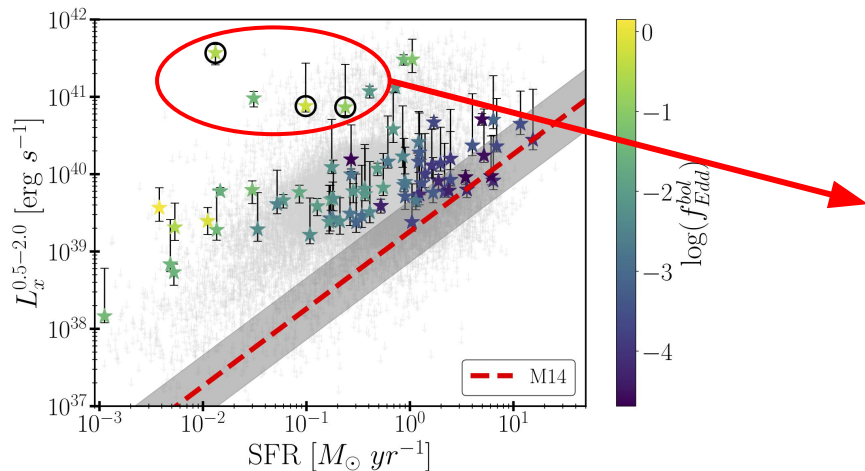
➤ L21 results in more luminous HMXBs in lower SFRs due to the lower metallicity.

➤ $\text{Prob}_{\text{stoch}} < 0.05\%$

Stochastic sampling is not adequate to explain the most X-ray luminous individual galaxies.

HEC-eR1 Normal Galaxy study

Lx excess: Low - luminosity AGNs or TDEs ?



If all the X-ray emission is due to accretion onto a SMBH how much powerful is it ?

$$M_{\star} \rightarrow M_{\text{BH}} \rightarrow L_{\text{Edd}} \rightarrow f_{\text{Edd}}^{\text{Bol}} \text{ is typical of Seyfert 1}$$

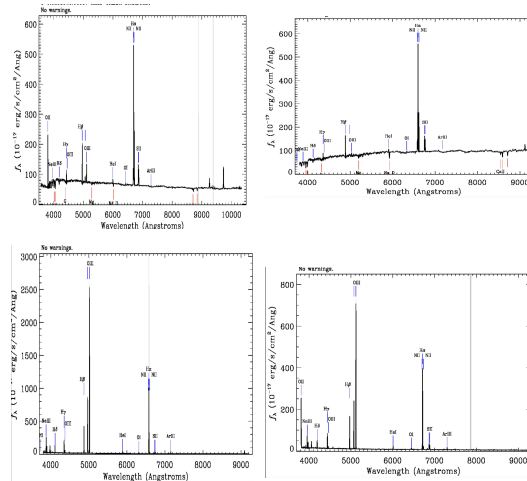
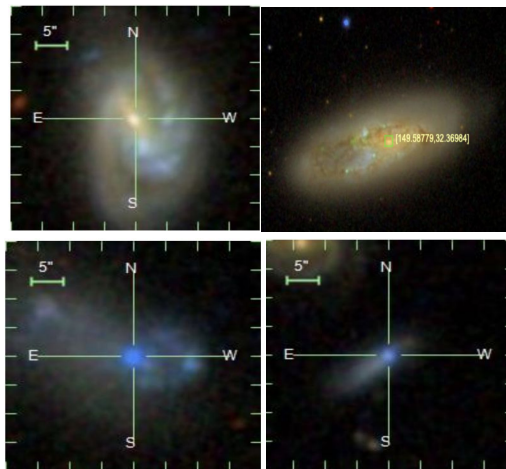
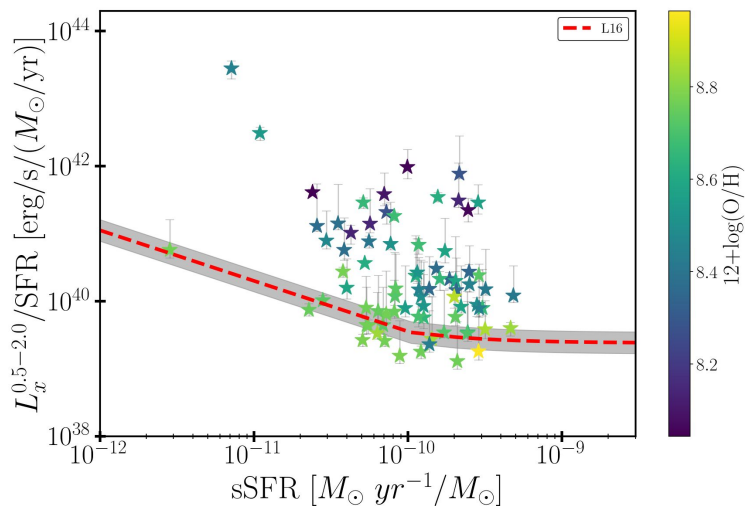
Are there **AGN signatures** in their **optical spectra** ?

Tidal Disruption Events ?

TDE rate for SFGs x eR1-HEC sample of SFGs \sim **0.04 TDE yr^{-1}** or Prob. of observing \sim **1%**

HEC-eR1 Normal Galaxy study

Lx excess: Finally what ?



- ★ A subpopulation of galaxies with **high sSFRs**, **lower metallicities** & **very young stellar populations** due to a recent star-formation episode.

HEC-eR1 Normal Galaxy study

Conclusions

1. The 1st X-ray unbiased all-sky survey of star-forming galaxies with eROSITA.
2. Redefined the L_x-SFR & L_x-SFR-Metallicity scaling relations accounting for intrinsic scatter.
3. Discovery of a population of extremely X-ray luminous star-forming galaxies:
 - a. Their star-forming nature is confirmed by their optical spectra.
 - b. Driver of the L_x excess: high sSFRs, lower metallicities & very young stellar population.
 - c. Stochasticity effects are very important.
4. Important implications for binary formation in low metallicity and high-z universe.
5. Stay tuned for updates based on eRASS:4.
 - a. Better X-ray statistics, more detections.
 - b. Extension to more distant lower metallicity galaxies.
 - c. Normal Galaxy XLFs.

Paper submitted to A&A, available at arXiv: 2402.12367

Contact: ekyritsis@physics.uoc.gr

